

Moderate Increase in *Mdr1a/1b* Expression Causes *In vivo* Resistance to Doxorubicin in a Mouse Model for Hereditary Breast Cancer

Marina Pajic,¹ Jayasree K. Iyer,¹ Ariena Kersbergen,¹ Eline van der Burg,¹ Anders O.H. Nygren,² Jos Jonkers,¹ Piet Borst,¹ and Sven Rottenberg¹

¹Division of Molecular Biology and Centre for Biomedical Genetics, The Netherlands Cancer Institute;

²MRC-Holland, Amsterdam, The Netherlands

Abstract

We have found previously that acquired doxorubicin resistance in a genetically engineered mouse model for BRCA1-related breast cancer was associated with increased expression of the mouse multidrug resistance (*Mdr1*) genes, which encode the drug efflux transporter ATP-binding cassette B1/P-glycoprotein (P-gp). Here, we show that even moderate increases of *Mdr1* expression (as low as 5-fold) are sufficient to cause doxorubicin resistance. These moderately elevated tumor P-gp levels are below those found in some normal tissues, such as the gut. The resistant phenotype could be completely reversed by the third-generation P-gp inhibitor tariquidar, which provides a useful strategy to circumvent this type of acquired doxorubicin resistance. The presence of MDR1A in drug-resistant tumors with a moderate increase in *Mdr1a* transcripts could be shown with a newly generated chicken antibody against a mouse P-gp peptide. Our data show the usefulness of realistic preclinical models to characterize levels of *Mdr1* gene expression that are sufficient to cause resistance. [Cancer Res 2009;69(16):6396–404]

Introduction

The anthracycline doxorubicin is frequently used in standard adjuvant, neoadjuvant, or palliative chemotherapy regimens for breast cancer patients (1). Doxorubicin increases the levels of (double-stranded) DNA breaks resulting in cell death. Spontaneous mammary tumors deficient in the error-free homology-directed repair of DNA damage are especially sensitive to this drug (2). However, successful chemotherapy of breast cancer is hampered by the development of multidrug resistance. As underlying cause, a range of different mechanisms has been identified, including alterations in drug target, drug accumulation/metabolism, DNA repair, or cell death pathways (3–6). For several of these mechanisms, their relevance to resistance in real tumors is sparse (7–10). One of the best-characterized mechanisms of multidrug resistance *in vitro* is drug efflux by ATP-binding cassette (ABC) transporters such as ABCB1/MDR1/P-glycoprotein (P-gp), ABCG2/BCRP, or ABCC1/MRP1 (3). P-gp is present in the apical membrane

of many different normal cells and its substrate specificity is broad (11, 12). Nevertheless, whether P-gp is relevant for clinical multidrug resistance of breast cancers is still debated (13–15). One issue that feeds the argument is the difficulty to detect P-gp *in situ* using formalin-fixed tumor samples. Another issue is that inhibitors of P-gp have only yielded a modest benefit in the clinic. First-generation, nonspecific inhibitors, such as verapamil and cyclosporine A, did not reach clinically effective plasma levels necessary for P-gp inhibition (16). Second-generation inhibitors, such as PSC 833 (valsopodar), were more potent and selective, but their pharmacokinetic interactions with drugs often necessitated reductions of doses of the anticancer drugs. A more selective third-generation P-gp inhibitor is tariquidar (XR9576, Avaant; ref. 17). In several studies, no clinically relevant interactions with pharmacokinetics of agents such as doxorubicin, vincristine, paclitaxel, or vinorelbine were detected, although (moderate) increases in chemotherapy side effects were observed in patients (18).

We have recently investigated anticancer drug responses in a genetically engineered mouse model for hereditary breast cancer (*K14cre;Brca1^{F/F};p53^{F/F}*; refs. 2, 19). Mammary tumors that spontaneously develop in this model mimic key features of breast cancer 1 (BRCA1)-associated mammary carcinomas in humans. An advantage of this mouse model is that these features as well as the individual tumor gene expression profiles are preserved on orthotopic grafting of small tumor fragments into syngeneic mice. Because BRCA1 is essential for the repair of double-stranded DNA breaks by homologous recombination, it is not surprising that the *Brca1^{-/-}/p53^{-/-}* tumors tested were sensitive to the DNA-interacting drugs cisplatin, doxorubicin (2), topotecan,³ and carboplatin or the poly(ADP-ribose) polymerase inhibitor AZD2281 (20, 21). Nevertheless, tumors could not be eradicated and eventually acquired resistance to each of the drugs tested, with the exception of cisplatin and carboplatin. A major mechanism of acquired doxorubicin and AZD2281 resistance in these tumors was increased expression of the *Mdr1a* and *Mdr1b* (in short *Mdr1*) genes, which encode the murine drug-transporting P-gp. High *Mdr1* expression was associated with increased washout of the P-gp substrate ^{99m}Tc-sestamibi and cross-resistance to the taxane docetaxel (2). Intriguingly, we found only low (~5-fold) increases of *Mdr1* transcripts in some tumors and wondered whether these were sufficient to explain the resistant phenotype.

Here we report that a ~5-fold increase above the average *Mdr1a* and *Mdr1b* transcript levels of untreated tumors is sufficient to cause doxorubicin resistance. Such amounts are far below

Note: Supplementary data for this article are available at Cancer Research Online (<http://cancerres.aacrjournals.org/>).

Request for reprints: Sven Rottenberg, Division of Molecular Biology and Centre for Biomedical Genetics, The Netherlands Cancer Institute, Plesmanlaan 121, 1066 CX Amsterdam, The Netherlands. Phone: 31-205122082; Fax: 31-206691383; E-mail: s.rottenberg@nki.nl.

©2009 American Association for Cancer Research.
doi:10.1158/0008-5472.CAN-09-0041

³ S.A.L. Zander, P. Borst, and S. Rottenberg, unpublished.

transcript quantities found in normal tissues such as the gut (*Mdr1a*) or kidney and adrenals (*Mdr1b*). In several tumors showing a moderate increase in *Mdr1* gene expression, P-gp levels could be detected with a newly generated polyclonal antibody.

Materials and Methods

Animals, generation of mammary tumors, and orthotopic transplantations into syngeneic wild-type mice. Doxorubicin-sensitive and doxorubicin-resistant *Brcal*^{-/-};*p53*^{-/-} mammary tumors were generated in *K14cre;Brcal*^{F/F};*p53*^{F/F} mice, genotyped, and orthotopically transplanted as described (2, 22). Starting 2 weeks after tumor grafting, the onset of tumor growth was checked at least three times a week. Mammary tumor size was determined by caliper measurements (length and width in mm) and tumor volume (in mm³) was calculated using the following formula: $0.5 \times \text{length} \times \text{width}^2$. Animals were euthanized with CO₂ when the tumor volume reached 1,500 mm³. In addition to sterile collection of multiple tumor pieces for grafting experiments, tumor samples were snap frozen in liquid nitrogen and fixed in 4% formalin. All experimental procedures on animals were approved by the Animal Ethics Committee of the Netherlands Cancer Institute.

Drugs. Doxorubicin (Adriablastina; Pharmacia Netherlands) was diluted to 1 mg/mL in saline (Braun). Tariquidar (Avaant) was diluted in 5% glucose such that the final volume administered by i.p. injection was 10 μL/g of body weight.

Treatment of mammary tumor-bearing animals. When mammary tumors reached a size of ~200 mm³, 5 mg doxorubicin was given i.v. on day 0. Controls were left untreated. To avoid accumulating toxicity of repeated drug injections, an additional treatment was not given after the recovery time of 7 days when the tumor responded to the treatment (tumor size <50% of the original volume, partial response). In this case, treatment was resumed once the tumor relapsed to its original size (100%). For tumors with a volume ≥50% after the recovery time, an additional treatment with the same dose as mentioned above was given.

Multiplex ligation-dependent probe amplification analysis. Total RNA and DNA were isolated from snap frozen tumor samples with Trizol (Invitrogen) according to the manufacturer's protocol. Multiplex ligation-dependent probe amplification (MLPA) reactions on DNA samples were done as described⁴ and the employed oligos are indicated in Supplementary Table S1. The integrity of RNA was verified by denaturing gel electrophoresis. For RNA quantification, reverse transcription-MLPA analysis comprising reverse transcription, hybridization, ligation, PCR amplification, and fragment analysis by capillary electrophoresis was done as described (2). To detect *hypoxanthine phosphoribosyltransferase 1* (*Hprt1*), we used CAGGTCAGCAAAGAAGCT as reverse transcription primer (5'-3') and TCCTCATGGACTGATTATGGACAGGACTGAAAG, ACTTGCTCGAGATGTCATGAAGGAGATGGGAGCCATCACA, and TTGTGGCCCTGTGTGCTCAAGGGGGGCTAT (5'-3') as target-specific sequences for the ligation reaction. For *β₂-microglobulin*, CTGCGTGCATAAATTGTATAG (5'-3') was used in the reverse transcription reaction and CATGTGATCAAGCATCATGATGCTCTGAA and GATTCATTTGAACCTGCTTAATTACAAATC-CAGTTTCTAATATG (5'-3') for the ligation step.

5'-Rapid amplification of cDNA ends. Total RNA was extracted from four doxorubicin-resistant tumors and four untreated tumors. RNA was quantified, and a standard 5'-rapid amplification of cDNA ends (5'-RACE) protocol was done to determine the transcriptional start site of *Mdr1a* and *Mdr1b* transcripts. The Generacer kit was obtained from Invitrogen, and 5'-RACE was done as per the manufacturer's instructions. Primers were designed to be within coding regions near the ATG start site. RACE products were cloned into TOPO TA vector (Invitrogen) and transformed into bacteria. Multiple clones (at least 20 for each 5'-RACE experiment) were sequenced to build a repertoire of transcribed mRNA sequences expressed

in each tumor. RACE primers (5'-3'): gene-specific primer *Mdr1a*: MseMdr1a JM5: CTTCCTTAAGGTCTCTTCAAGTCC, nested primer *Mdr1a*: MseMdr1a JM6: AAGTTCATCAGACCTCACGTGTCTTACC, gene-specific primer *Mdr1b*: MseMdr1b JM7: GAACGTGAAATAATTTGGC-TACCTCTTTTGCCC, nested primer *Mdr1b*: MseMdr1b nest JM8: TCTGCTTCCCTTAAGGTTCTCTTCAAATCC. To set up the procedure, we used the vinblastine-selected mouse macrophage cell lines J774.2 and J7.V1 described by Greenberger and colleagues (23) and kindly provided by C.P.H. Yang and Dr. Susan B. Horowitz (Albert Einstein College of Medicine).

Western blot analysis. Tumor samples were homogenized in 10 mmol/L KCl, 1.5 mmol/L MgCl₂, 10 mmol/L Tris-HCl (pH 7.4), and 0.5% (w/v) SDS supplemented with Complete protease inhibitors (Roche). DNA was sheared by sonication, and samples containing 50 μg protein were fractionated by SDS-PAGE on a 7.5% Tris-glycine gel and then transferred onto a nitrocellulose membrane by electroblotting. After blotting, the membranes were blocked for at least 1 h in TBS (10 mmol/L Tris, 100 mmol/L NaCl) containing 5% milk powder and 0.05% Tween followed by an overnight incubation at 4°C with the C219 antibody at 1.2 μg/mL. Immunoreactivity was visualized with horseradish peroxidase-conjugated rabbit anti-mouse immunoglobulins (DakoCytomation; diluted 1:5,000) followed by enhanced chemiluminescence detection.

LS9509 antibody. The sequences for mouse *Mdr1a* and *Mdr1b* genes were analyzed by the algorithm of Hopp and Woods to determine potential peptides for synthesis and antibody production. The peptides were then BLASTed against the Swiss-Prot database to determine uniqueness and to help predict the specificity of the resulting antibodies. Peptide KMGKSKKEKKEKPAVSV was selected and synthesized, and chicken polyclonal antisera were generated at Lifespan Biosciences. To allow for peptide conjugation to the carrier protein, a cysteine residue was added to the NH₂ terminus of the peptides. The 77-day yolks were subjected to peptide affinity purification, and the resulting antisera were then used as primary antibody, termed LS9509.

Immunocytochemistry. LLC-PK1 and its corresponding P-gp-transfected lines grown on slides were fixed with -20°C acetone for 40 s and incubated in serum-free protein block (DakoCytomation) for 1 h. The cells were then incubated overnight with PBS containing 1% bovine serum albumin and a primary antibody, which was either LS9509 or C219 (Calbiochem) at a final protein concentration of 0.26 or 2.9 μg/mL, respectively. Slides were washed with PBS followed by subsequent incubation with a biotin-coupled appropriate secondary antibody for 1 h at a dilution of 1:1,000 (v/v) and a streptavidin-horseradish peroxidase conjugate (Vector Laboratories) for 30 min at room temperature. Immunoreactions were visualized with diaminobenzidine (Sigma), and the sections were counterstained with hematoxylin.

Immunofluorescence on tissue sections. Freshly cut 4-μm-thick frozen sections of mouse tumor tissue were fixed with -20°C acetone for 10 min. Sections were then blocked for avidin/biotin (DakoCytomation) for 10 min and in serum-free protein block (DakoCytomation). For C219 immunofluorescence, additional blocking steps were introduced to remove nonspecific interactions with mouse-on-mouse block (M.O.M kit; Vector Laboratories) according to the manufacturer's instructions. The tissue sections were then incubated overnight at 4°C with primary antibodies (0.26 μg/mL for the LS9509 antibody or 11.6 μg/mL for the C219 antibody). Slides were washed with PBS followed by subsequent incubation with a biotin-coupled appropriate secondary antibody for 1 h at a dilution of 1:1,000 (v/v) and a 30-min incubation with streptavidin-Cy5 (Invitrogen) at a dilution of 1:50 (v/v) and finally a 5-min incubation with 4',6-diamidino-2-phenylindole to stain the nuclei. The slides were washed with PBS as described above and mounted in Vectashield mounting medium (Molecular Probes). The Cy5 and 4',6-diamidino-2-phenylindole fluorescence in the tissue sections was analyzed with a Leica confocal AOBs fluorescence microscope.

Results

Doxorubicin resistance of *Brcal*^{-/-};*p53*^{-/-} tumors with a moderate increase of *Mdr1a/Mdr1b* expression can be reversed by the P-gp inhibitor tariquidar. In addition to

⁴ <http://www.mrc-holland.com>

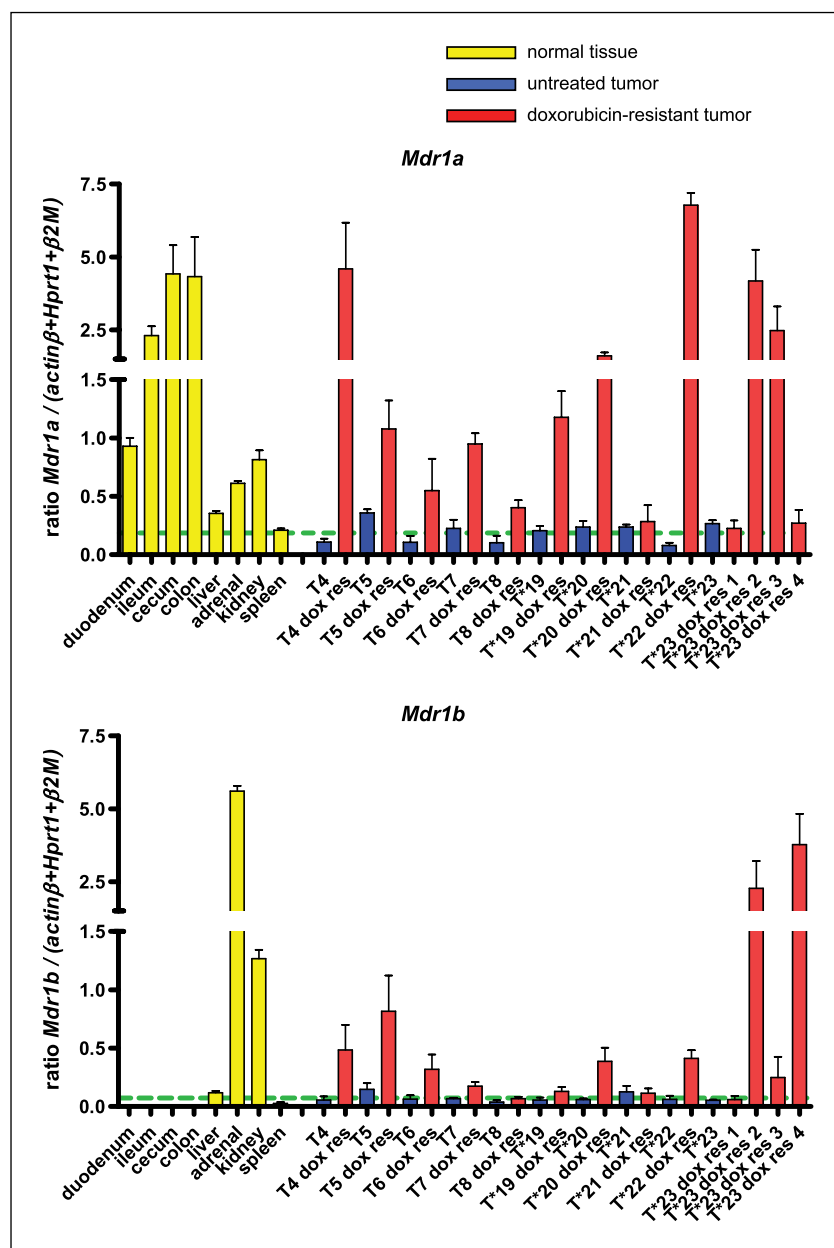


Figure 1. Comparison of *Mdr1* mRNA levels with those found in normal tissues. Reverse transcription-MLPA analysis of the ratios of *Mdr1a* and *Mdr1b* expression in normal tissues (yellow), doxorubicin-resistant tumors (red), and samples from the corresponding untreated tumors (blue). The sum of *actin* β , *Hprt1*, and β_2 -microglobulin (β_2M) expression was used as reference. Green dotted lines, average *Mdr1a*/*(actin* β +*Hprt1*+ β_2M) and *Mdr1b*/*(actin* β +*Hprt1*+ β_2M) ratios (0.19 and 0.072) found in the untreated tumors. Columns, mean ratio of three reactions; bars, SD.

published ratios of resistant tumors versus matched samples taken before treatment (2), we determined *Mdr1* gene expression levels in doxorubicin-sensitive and doxorubicin-resistant mouse mammary tumors in comparison with selected normal tissues by reverse transcription-MLPA. *actin* β , *Hprt1*, and β_2 -microglobulin were used as reference and relative *Mdr1* transcript levels were compared with those of the liver, gut, adrenals, and kidney, which are known to express P-gp. As shown in Fig. 1, the average level of *Mdr1* RNA in untreated tumors was comparable with that of the spleen. Intriguingly, tumor 5 (T5), which has a 1.9- and 2.0-fold higher RNA level than the average *Mdr1a* and *Mdr1b* of untreated tumors, showed a stable disease in response to doxorubicin, whereas the other tumors usually shrank in response to treatment (2). In the resistant tumors, at least 2-fold increased *Mdr1* RNA levels above the *Mdr1* average of untreated tumors were detected in 11 of 13 tumors (Fig. 1; Supplementary Table S2). *Mdr1a* transcript levels

varied between those reached in the liver (T6doxres and T8doxres, 2- to 3-fold above the average of untreated tumors), duodenum (T5doxres, T7doxres, and T*19doxres, 5- to 6-fold above the average of untreated tumors), and ileum and large intestine (T*4doxres, T*20doxres, T*22doxres, T*23doxres2, and T*23doxres3, up to 36-fold above the average of untreated tumors). Regarding *Mdr1b* transcripts, only in two tumors (T*23doxres2 and T*23doxres4) levels between those found in the kidney or adrenal glands were measured (31- to 52-fold above the average of untreated tumors), but none reached those found in the adrenal gland. In summary, only one doxorubicin-resistant tumor (T*22doxres) had higher *Mdr1* RNA levels than some normal tissues.

On orthotopic transplantation into syngeneic animals, doxorubicin-resistant tumors kept their resistance phenotype or showed only a slight delay in growth in the presence of doxorubicin (ref. 2; Fig. 2), whereas the primary sensitive tumors shrank substantially

(2). To determine the importance of P-gp in doxorubicin-resistant tumors, we pretreated the mice with the P-gp inhibitor tariquidar (17). When 10 mg tariquidar/kg i.v. was given 15 min before doxorubicin, animals could only tolerate four to five subsequent treatments of the MTD of doxorubicin (5 mg/kg i.v., minimally 7 days recovery time). This is less than what can be administered when doxorubicin is given as single agent (at least eight cycles are usually tolerated). Histologic analysis of sacrificed animals after repeated doxorubicin + tariquidar doses revealed bone marrow depletion as the most likely cause of toxicity (data not shown). After the initial injection on day 0 (volume ~200 mm³), additional treatments were given 7 days later in case the tumor size was >50% of the size on day 0. In case the tumor regressed to a size below 50%, we resumed treatment when the tumor relapsed to 100%. As shown in Fig. 2, P-gp inhibition successfully reversed doxorubicin resistance in three individual tumors in which we found increased *Mdr1* mRNA levels. T*23doxres1, in which no *Mdr1* increase was observed (Fig. 1), showed only a small benefit of the pretreatment with tariquidar. Despite the fact that tumors became sensitive

again to doxorubicin, they were not eradicated by the tariquidar-doxorubicin combination.

Up-regulation of *Mdr1* is not caused by gene amplification in most tumors and does not correlate with differential promoter usage of *Mdr1a* or *Mdr1b*. Amplification of *MDR1* or its rodent homologues has been observed in many multidrug-resistant cell lines (reviewed in ref. 4). In contrast, we found no increase in the DNA content of 12 of 13 doxorubicin-resistant tumors relative to samples taken before tumor treatment (Supplementary Fig. S1). Only for T*23doxres4 a 1.8-fold increase was identified. However, a small increase in *Mdr1* copy number might be difficult to detect in crude tumor samples. We therefore enriched tumor cells from two doxorubicin-resistant tumors (T*23doxres2 and T7doxres) by removing dead cells, endothelial, fibroblastic, and hematopoietic (Lin⁺) cells after tumor dissociation. MLPA analysis of these Lin⁻ cells did not detect any *Mdr1* amplification (Supplementary Fig. S2). These results suggest that increased transcription of *Mdr1* rather than gene amplification drives the increased *Mdr1* expression in most of the tumors.

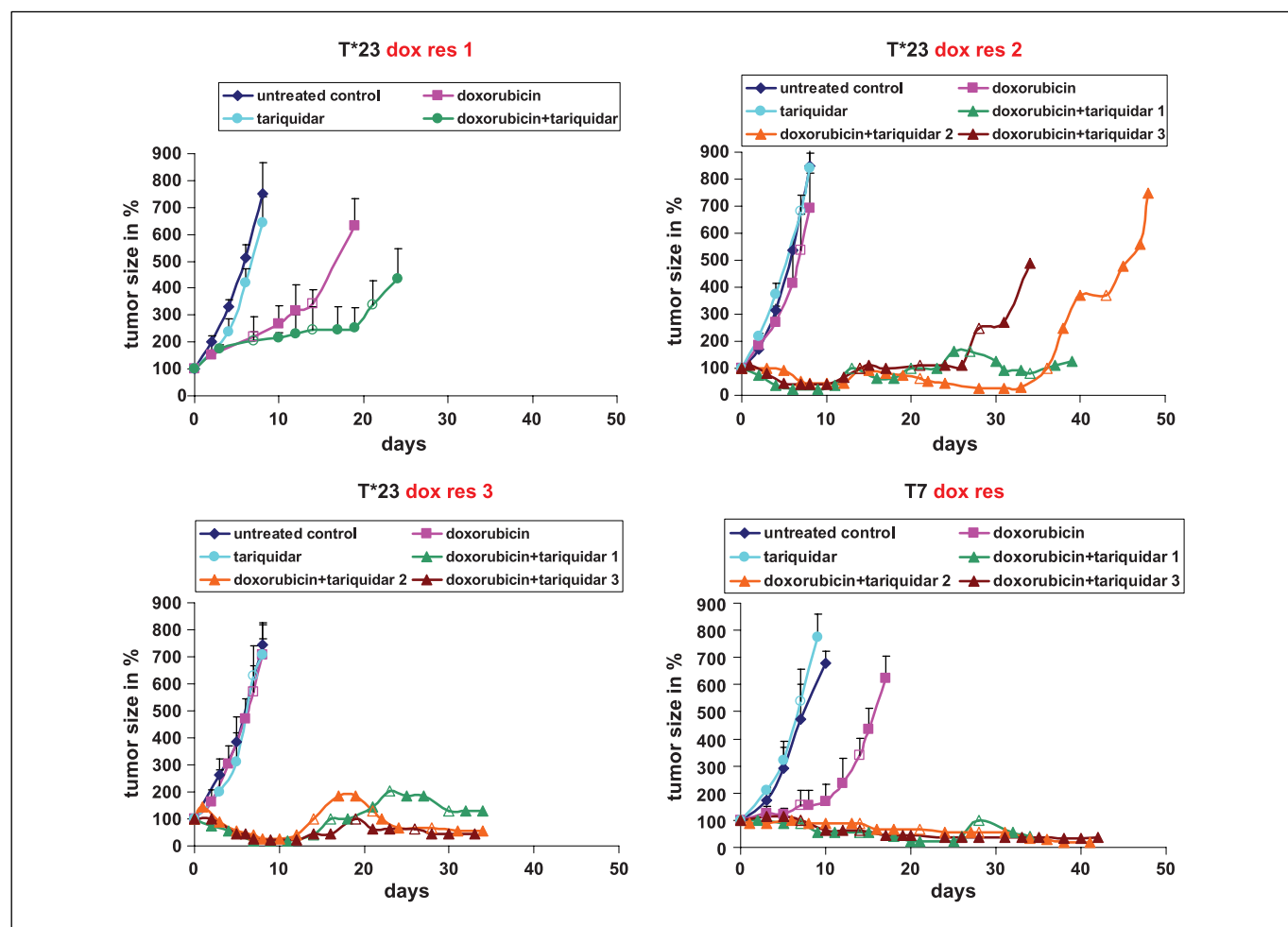


Figure 2. Response of doxorubicin-resistant tumors to doxorubicin combined with tariquidar. Fragments of doxorubicin-resistant tumors with different increases of *Mdr1* transcripts (T*23doxres2, T*23doxres3, and T7doxres) or without detectable *Mdr1* mRNA alterations (T*23doxres1) were transplanted orthotopically into syngeneic mice and left untreated (dark blue) or treated with 10 mg tariquidar/kg i.v. (turquoise), 5 mg doxorubicin/kg i.v. (pink), or 10 mg tariquidar/kg i.v. followed 15 min later by 5 mg doxorubicin/kg i.v. (green, orange, and brown). In case tumors did not shrink <50%, animals were retreated after a recovery time of 7 d. Days on which animals were retreated are indicated (open circles, triangles, or squares). Where error bars (SD) are given, the data points represent the mean of three individual animals. Due to the variability of relapsing tumors after tariquidar-doxorubicin combinations, the three individual curves are presented for T*23doxres2, T*23doxres3, and T7doxres.

Two types of transcriptional activation of the human *MDR1* gene have been reported in human tumor samples and cell lines: DNA rearrangements linking the *MDR1* gene to a strong promoter (24, 25) and activation of a “distal” promoter, 100 kb upstream of the *MDR1* gene (26, 27). In mouse cell lines, *Mdr1* gene activation may also occur by (defective) retrovirus insertion (28) or by DNA rearrangements proposed to result from unequal sister chromatid exchange mediated by LINE-1 repetitive elements (29). To test whether any of these mechanisms apply in our resistant tumors, we mapped the start of *Mdr1a* and *Mdr1b* transcripts using a 5'-RACE protocol, which allows cloning of 5'-cap-linked sequences. The results obtained for the capped transcripts of four individual doxorubicin-resistant tumors and their matched doxorubicin-sensitive controls are presented in Fig. 3. Both for *Mdr1a* and *Mdr1b* we find a range of transcripts starting at a proximal promoter, 132 to 186 nucleotides upstream of the ATG in the case of *Mdr1a* and 116 to 186 nucleotides for *Mdr1b*. These start sites approximately coincide with transcriptional start positions found previously for *Mdr1a* (30, 31) and *Mdr1b* (32, 33) in cell lines and normal tissues. In our model, there is no obvious difference between the exact start sites of resistant and sensitive tumors.

For *Mdr1a*, we also find transcripts starting far upstream of the gene. We find these in four individual tumors, all starting at position 8567101 bp of chromosome 5.⁵ Remarkably, in this limited analysis of a small number of tumors, we see no correlation between the use of this distal promoter and *Mdr1a* up-regulation. In two drug-sensitive tumors (T*20 and T*22) and one drug-resistant tumor without detectable *Mdr1a* up-regulation (T*23doxres4), we find a transcript from the distal promoter, whereas among the three tumors with *Mdr1a* up-regulation we only see a distal promoter transcript in T4doxres. Even from this limited set of tumors, it is clear that the up-regulation of *Mdr1a* is not specifically associated with activation of a distal promoter in our mouse mammary tumors, in contrast to what was observed in human tumors/cell lines (26, 34). A distal promoter for *Mdr1a*, not identical to the one identified here, has only been found in one set of vinblastine-selected mouse macrophage cell lines (30).

Detection of MDR1A with a new mouse-specific antibody. We determined the amount of P-gp by Western blotting and/or immunofluorescence with a range of mouse- and human-specific antibodies such as C219 (Calbiochem), 265/F4, 4E3, Ab36743, and SPM137 (all from Abcam), NH211 (35), 15D3 (36), and UIC2 (Chemicon). Of the antibodies tested, the C219 monoclonal antibody (37), which is one of the most frequently used to detect human and mouse P-gp (38, 39), was the most sensitive in detecting mouse MDR1A and MDR1B in LLC-PK1 polarized pig kidney cells transfected with the *Mdr1* genes (ref. 40; Supplementary Figs. S3 and S4). In tumors with at least 25-fold higher *Mdr1* transcripts than untreated tumors (T4doxres, T*22doxres, T*23doxres2, and T*23doxres4), P-gp was detected by Western blotting using C219 (Supplementary Fig. S3), although this antibody also bound nonspecifically to other proteins, as indicated by multiple bands. In several tumors with a moderate increase in *Mdr1* expression (T5doxres, T6doxres, T7doxres, and T*23doxres3), however, we did not detect clearly more P-gp than in the untreated doxorubicin-sensitive tumors (T1, T2, T*22con, and T*23con).

To improve the detection of mouse P-gp *in situ*, we raised a new chicken polyclonal antibody using the peptide KMGKKSKEK-KEKKPAVSV, which corresponds to amino acids 17 to 35 of mouse MDR1A (accession no. NP_035206). This NH₂-terminal sequence has a high homology to mouse MDR1B (18 of 19) and human MDR1 (16 of 19). In our search for suitable peptides, we avoided extracellular loops due to their increased risk of yielding conformation-specific antibody binding. Moreover, we chose KMGKKSKEKKEKKPAVSV to avoid cross-reaction with MDR3/ABC4, as this complicates the use of C219, which reacts with the core sequence VQEALD also present in ABC4 (41, 42). When we tested the resulting affinity-purified polyclonal LS9509 antibodies on the transfected LLC-PK1 cells, only MDR1A could be detected by immunocytochemistry, whereas MDR1B and human MDR1 were not identified (Fig. 4A). Unfortunately, this antibody did not yield a positive result on Western blot (data not shown). To evaluate the suitability of LS9509 for immunostaining, we compared brain sections of *Mdr1* wild-type animals with those derived from *Mdr1*^{-/-} animals (43). As illustrated in Fig. 4B, LS9509 stained brain capillaries in wild-type but not in knockout animals. When we probed our panel of doxorubicin-resistant tumors with LS9509, we found that more tumors yielded plasma membrane staining than with the C219 antibody (Supplementary Table S3): all tumors with high levels of *Mdr1a* transcripts (T4doxres, T*22doxres, and T23*doxres2) were positive. Of tumors with moderate increase in *Mdr1a*, T5doxres, T7doxres, T*19doxres, T*20doxres, and T*23doxres3 showed positive staining, whereas all other doxorubicin-resistant tumors were negative. Figure 4C shows representative examples of T*22doxres, T23*doxres2, and T5doxres with corresponding controls. These results show that P-gp is indeed expressed in tumors with a moderate transcriptional up-regulation of *Mdr1*.

Discussion

In this study, we show that moderate increases in the expression of *Mdr1* genes encoding P-gp are sufficient to cause acquired doxorubicin resistance in a realistic mouse model for BRCA1-associated breast cancer. In several resistant tumors, *Mdr1* mRNA levels were only 5- to 13-fold above the average of *Mdr1a* or *Mdr1b* in untreated tumors. The levels in the resistant tumors are comparable with those found in the liver or duodenum of wild-type mice and we rarely found tumor levels exceeding those normally found in the large intestine (*Mdr1a*) or kidneys (*Mdr1b*). In normal tissues, reduced doxorubicin sensitivity has also P-gp-independent causes such as lack of proliferation or intact DNA repair mechanisms. In the investigated tumors, we are confident that these low levels of P-gp cause doxorubicin resistance, as resistance could be reversed by the third-generation P-gp inhibitor tariquidar. We conclude that in our tumor model P-gp plays a pivotal role in causing drug resistance even in tumors with only a 5-fold increase in *Mdr1a* and *Mdr1b* mRNA. Our inability to eradicate tumors by the tariquidar-doxorubicin combination might be due to dormancy of residual tumor-initiating cells or other mechanisms (44).

Thus far, it has been difficult to show a role for P-gp in drug-resistant breast cancer *in vivo*. As an example, a meta-analysis of 31 breast cancer trials found P-gp expression in 41% of the tumors and associated a 3-fold chemotherapy response reduction with the presence of P-gp (45). Nevertheless, such studies need to be taken with a grain of salt due to huge differences in the definition of what

⁵ http://www.ensembl.org/Mus_musculus

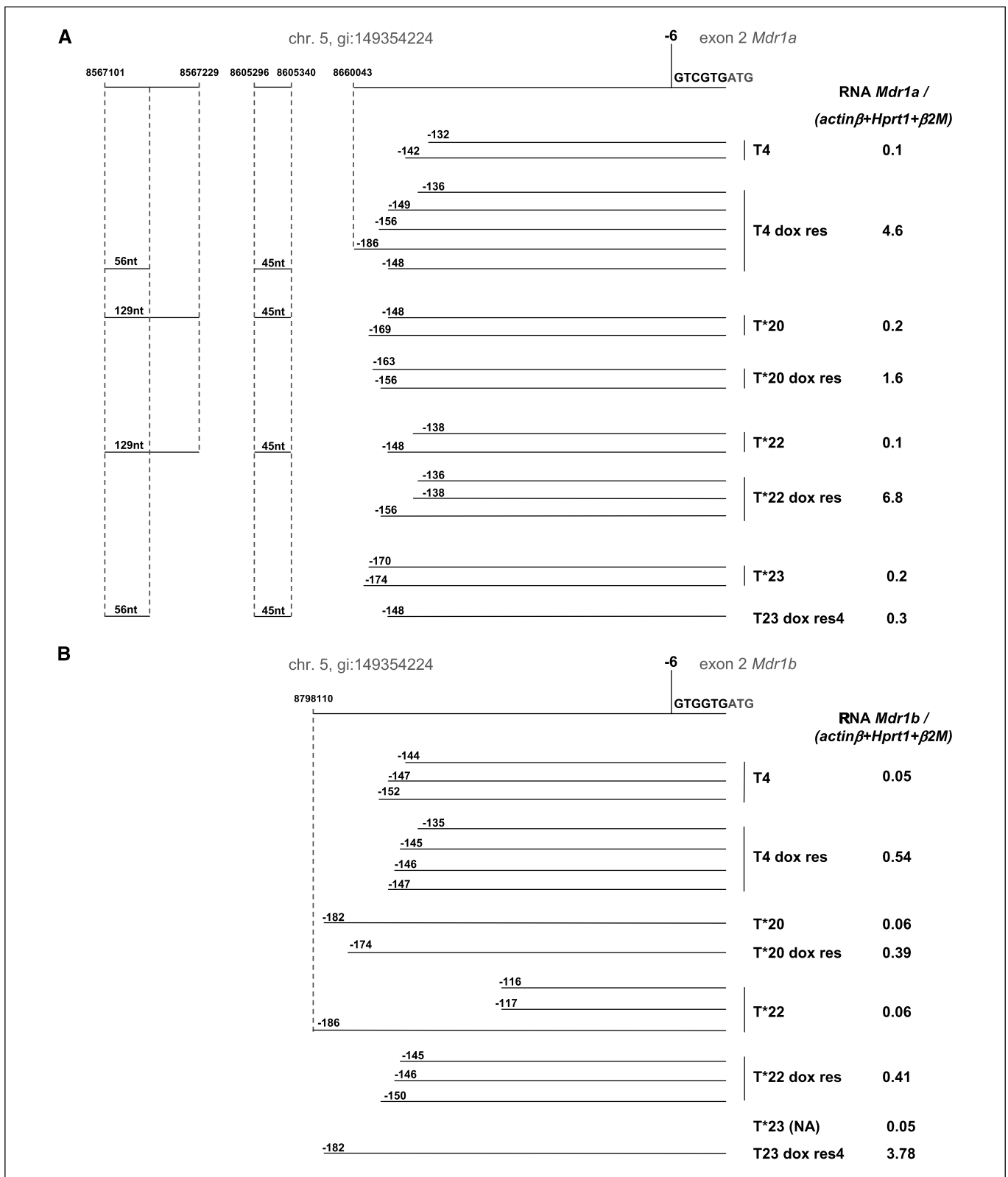


Figure 3. *Mdr1* 5'-RACE of doxorubicin-resistant and matched doxorubicin-sensitive tumors. **A**, *Mdr1a* products aligned to the sequence of *Mdr1a*. Numbers (in nucleotides; *nt*) indicate that each tumor (sensitive or resistant) expresses transcripts of various 5'-untranslated region lengths. The long transcripts match to regions containing canonical splice sites far upstream of the ATG start site, indicating that a distal transcriptional start site is used. All tumors (doxorubicin-resistant and doxorubicin-sensitive) express transcripts that use either proximal transcription start sites or a mixture of proximal and distal transcriptional start sites. Levels of *Mdr1a* RNA derived from these tumors are normalized to *actinβ*, *Hprt1*, and β_2M . **B**, *Mdr1b* 5'-RACE products aligned to the sequence of *Mdr1b*. Numbers (in nucleotides) indicate that each tumor expresses transcripts of various 5'-untranslated region lengths. All tumors (doxorubicin-resistant and doxorubicin-sensitive) express *Mdr1b* transcripts that use a proximal transcription start site. Levels of *Mdr1b* RNA derived from these tumors are normalized to *actinβ*, *Hprt1*, and β_2M .

constitutes a "P-gp positive" tumor. More recently, in a phase II clinical trial, tariquidar showed limited ability to restore drug sensitivity in 17 women with stage III to IV breast cancer who progressed or had stable disease on anthracycline or taxane therapy (46). Only the patient with the greatest increase in ^{99m}Tc -sestamibi uptake, who also showed inducible P-gp expression, responded partially to tariquidar-containing therapy. Clearly, careful patient selection is necessary to increase potential benefit from P-gp-inhibiting therapy. *In vivo* imaging using the P-gp substrate ^{99m}Tc -sestamibi is one approach, and we also found increased sestamibi washout in our doxorubicin-resistant tumor

model (2, 47). However, this tracer is not completely P-gp-specific and other drug efflux pumps (e.g., MRP1; ref. 48) that are not inhibited by P-gp-specific transport blockers could give a false-positive result.

Another approach is *in situ* detection with P-gp-specific antibodies. Our attempts to generate a more sensitive antibody for staining mouse P-gp were partially successful: the new chicken-derived LS9509 antibody detects only mouse MDR1A *in situ*. Still, eight doxorubicin-resistant tumors, with at least 5-fold increased *Mdr1a* transcript levels relative to untreated tumors, were scored P-gp positive, whereas C219 detected P-gp only in one of these

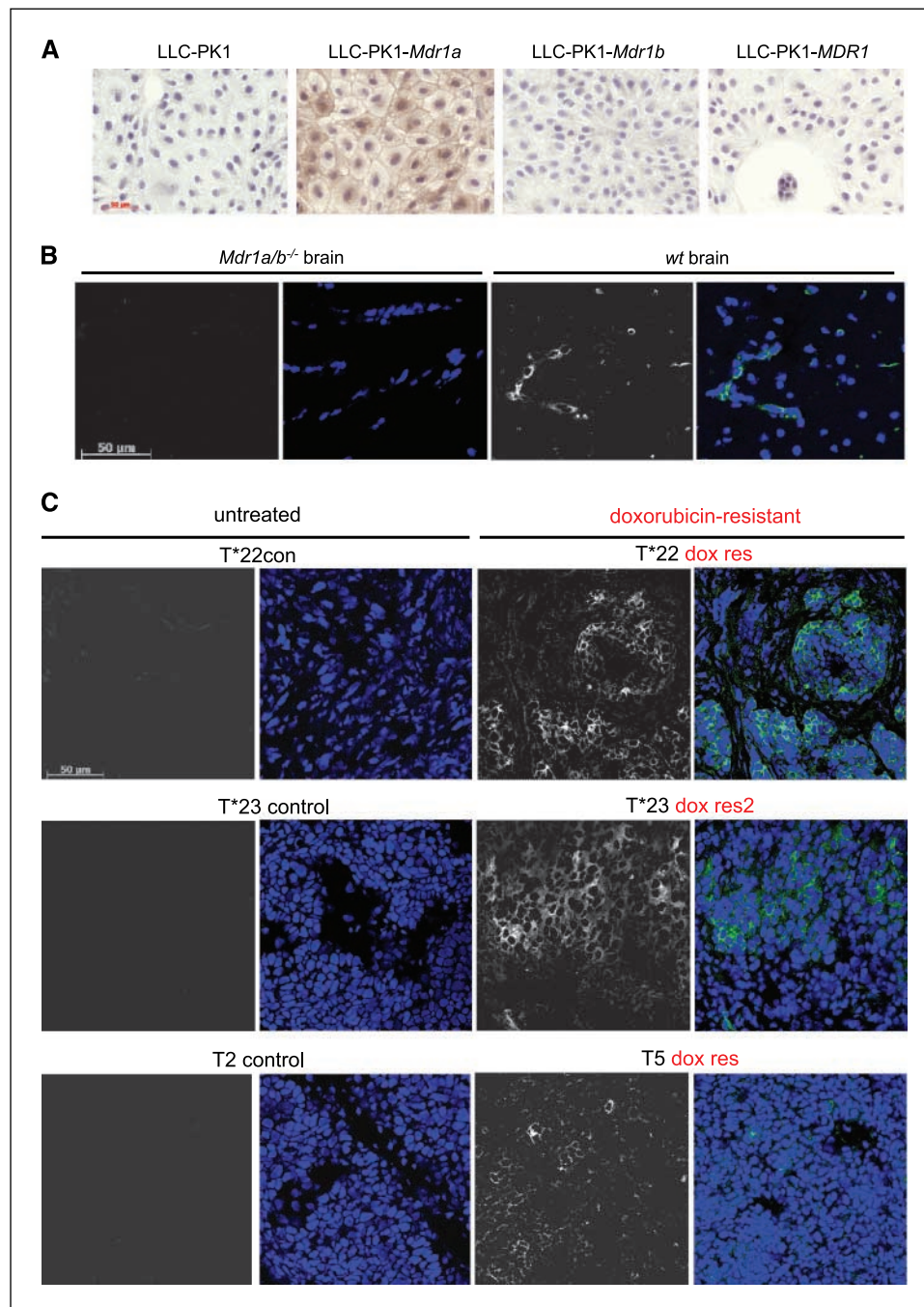


Figure 4. Analysis of doxorubicin-sensitive and doxorubicin-resistant tumors with the chicken polyclonal LS9509 antibody. **A**, LLC-PK1 polar porcine kidney cells transfected with mouse *Mdr1a*, *Mdr1b*, or human *MDR1* probed with LS9509 (brown). **B**, brain sections of wild-type (wt) or *Mdr1a/b*^{-/-} animals tested with the LS9509 antibody (white, columns 1 and 3; green, columns 2 and 4). Nuclei were stained with 4',6-diamidino-2-phenylindole (blue, columns 2 and 4). **C**, OCT snap-frozen tumor slides of untreated or doxorubicin-resistant tumors incubated with LS9509 (white, columns 1 and 3; green, columns 2 and 4). Nuclei were stained with 4',6-diamidino-2-phenylindole (blue, columns 2 and 4). All incubations were done with LS9509 antibody at a final concentration of 0.26 $\mu\text{g}/\text{mL}$.

tumors. Possibly, the use of the mouse-on-mouse block for C219 is responsible for its reduced sensitivity. Although it remains possible that other human-specific antibodies that lack mouse cross-reactivity do a better job on human samples, it may be useful to generate more sensitive tools to detect P-gp in tumor sections. Besides new antibodies that are sensitive for both immunohistochemistry and immunoblotting, signal amplification via a proximity ligation assay (49) is another option that could be tested and optimized in our model.

Although our model mimics key features of BRCA1-associated breast cancer, it does not represent the full heterogeneity of treatment responses observed in breast cancer. We did not observe intrinsic doxorubicin resistance of drug-naïve tumors, although stable or progressive disease is often found in response to anthracycline-containing chemotherapy in humans. To what extent increased P-gp expression contributes to primary chemotherapy resistance in human breast cancer patients remains questionable. The poor outcome of tamoxifen pretreatment in such patients (46) does not favor a key role for P-gp. An advantage of our mouse model is that we can breed in *Mdr1*-null alleles (43) to identify *Mdr1*-independent doxorubicin resistance mechanisms.

Future studies with *Mdr1*^{-/-};*Bcr1*^{-/-};*p53*^{-/-} tumors should reveal novel drug resistance mechanisms that may also be involved in human breast cancers where P-gp inhibition is not beneficial.

Disclosure of Potential Conflicts of Interest

A.O.H. Nygren is an employee of MRC-Holland, which markets the MLPA tests used in this article. The other authors disclosed no potential conflicts of interest.

Acknowledgments

Received 1/7/09; revised 5/8/09; accepted 6/3/09; published OnlineFirst 8/4/09.

Grant support: Dutch Cancer Society grants 2006-3566 (P. Borst, S. Rottenberg, and J. Jonkers) and 2005-3379 (P. Borst, R. Bernards, and R.L. Beijersbergen), European Union FP6 Integrated Project 037665-CHEMORES (P. Borst and S. Rottenberg), and Swiss Foundation for Grants in Biology and Medicine grant PBEB-104429 (S. Rottenberg).

The costs of publication of this article were defrayed in part by the payment of page charges. This article must therefore be hereby marked *advertisement* in accordance with 18 U.S.C. Section 1734 solely to indicate this fact.

We thank Alfred Schinkel for critical reading of the manuscript and Susan Bates (NIH) for providing tamoxifen, and we are grateful to Dr. Susan B. Horwitz (Albert Einstein College of Medicine) for supplying the cell lines overexpressing *Mdr1a* and *Mdr1b* used to set up the 5'-RACE protocol.

References

- DeVita VT, Jr., Hellman S, Rosenberg SA. Cancer, principles & practice of oncology. 6th ed. Philadelphia: Lippincott Williams & Wilkins, 2001. p. 3-3235.
- Rottenberg S, Nygren AOH, Pajic M, et al. Selective induction of chemotherapy resistance of mammary tumors in a conditional mouse model for hereditary breast cancer. *Proc Natl Acad Sci U S A* 2007;104:12117-22.
- Szakacs G, Paterson JK, Ludwig JA, Booth-Genthe C, Gottesman MM. Targeting multidrug resistance in cancer. *Nat Rev Drug Discov* 2006;5:219-34.
- Fojo T. Multiple paths to a drug resistance phenotype: mutations, translocations, deletions and amplification of coding genes or promoter regions, epigenetic changes and microRNAs. *Drug Resist Updat* 2007;10:59-67.
- Schmitt CA. Senescence, apoptosis and therapy—cutting the lifelines of cancer. *Nat Rev Cancer* 2003;3:286-95.
- Voorzanger-Rousselot N, Alberti L, Blay JY. CD40L induces multidrug resistance to apoptosis in breast carcinoma and lymphoma cells through caspase independent and dependent pathways. *BMC Cancer* 2006;6:75.
- Brown M, Wilson G. Apoptosis genes and resistance to cancer therapy: what do the experimental and clinical data tell us? *Cancer Biol Ther* 2007;2:477-90.
- Brown JM, Attardi LD. The role of apoptosis in cancer development and treatment response. *Nat Rev Cancer* 2005;5:231-7.
- Borst P, Jonkers J, Rottenberg S. What makes tumors multidrug resistant? *Cell Cycle* 2007;6:2782-7.
- Roninson IB, Broude EV, Chang B-D. If not apoptosis, then what? Treatment-induced senescence and mitotic catastrophe in tumor cells. *Drug Resist Updates* 2001;4:303-13.
- Devault A, Gros P. Two members of the mouse *mdr* gene family confer multidrug resistance with overlapping but distinct drug specificities. *Mol Cell Biol* 1990;10:1652-63.
- Ueda K, Cardarelli C, Gottesman MM, Pastan I. Expression of a full-length cDNA for the human "MDR1" gene confers resistance to colchicine, doxorubicin, and vinblastine. *Proc Natl Acad Sci U S A* 1987;84:3004-8.
- Pusztai L. Markers predicting clinical benefit in breast cancer from microtubule-targeting agents. *Annals of Oncology ESMO* 2007;18 Suppl 12:xi15-20.
- O'Driscoll L, Clynes M. Biomarkers and multiple drug resistance in breast cancer. *Curr Cancer Drug Targets* 2006;6:365-84.
- Faneyte IF, Kristel PM, van de Vijver MJ. Determining MDR1/P-glycoprotein expression in breast cancer. *Int J Cancer* 2001;93:114-22.
- Raderer M, Scheithauer W. Clinical trials of agents that reverse multidrug resistance. A literature review. *Cancer* 1993;72:3553-63.
- Mistry P, Stewart AJ, Dangerfield W, et al. *In vitro* and *in vivo* reversal of P-glycoprotein-mediated multidrug resistance by a novel potent modulator, XR9576. *Cancer Res* 2001;61:749-58.
- Fox E, Bates SE. Tariquidar (XR9576): a P-glycoprotein drug efflux pump inhibitor. *Expert Rev Anticancer Ther* 2007;7:447-59.
- Liu X, Holstege H, van der Gulden H, et al. Somatic loss of BRCA1 and p53 in mice induces mammary tumors with pathologic and molecular features of human BRCA1-mutated basal-like breast cancer. *Proc Natl Acad Sci U S A* 2007;104:12111-6.
- Rottenberg S, Jaspers JE, Kersbergen A, et al. High sensitivity of BRCA1-deficient mammary tumors to the PARP inhibitor AZD2281 alone and in combination with platinum drugs. *Proc Natl Acad Sci U S A* 2008;105:17079-84.
- Martin SA, Lord CJ, Ashworth A. DNA repair deficiency as a therapeutic target in cancer. *Curr Opin Genet Dev* 2008;18:80-6.
- Jonkers J, Meuwissen R, van der Gulden H, Peterse H, Van der Valk M, Berns A. Synergistic tumor suppressor activity of BRCA2 and p53 in a conditional mouse model for breast cancer. *Nat Genet* 2001;29:418-25.
- Greenberger LM, Lothstein L, Williams SS, Horwitz SB. Distinct P-glycoprotein precursors are overproduced in independently isolated drug-resistant cell lines. *Proc Natl Acad Sci U S A* 1988;85:3762-6.
- Mickley LA, Spengler BA, Knutsen TA, Biedler JL, Fojo T. Gene rearrangement: a novel mechanism for MDR-1 gene activation. *J Clin Invest* 1997;99:1947-57.
- Mickley LA, Lee J-S, Weng Z, et al. Genetic polymorphism in MDR-1: a tool for examining allelic expression in normal cells, unselected and drug-selected cell lines, and human tumors. *Blood* 1998;91:1749-56.
- Chen KG, Wang YC, Schaner ME, et al. Genetic and epigenetic modeling of the origins of multidrug-resistant cells in a human sarcoma cell line. *Cancer Res* 2005;65:9388-97.
- Scotto KW. Transcriptional regulation of ABC drug transporters. *Oncogene* 2003;22:7496-511.
- Lepage P, Devault A, Gros P. Activation of the mouse *mdr3* gene by insertion of retrovirus in multidrug-resistant P388 tumor cells. *Mol Cell Biol* 1993;13:7380-92.
- Cohen D, Higman SM, Hsu SI, Horwitz SB. The involvement of a LINE-1 element in a DNA rearrangement upstream of the *mdr1a* gene in a Taxol multidrug-resistant murine cell line. *J Biol Chem* 1992;267:20248-54.
- Hsu SI, Cohen D, Kirschner LS, Lothstein L, Hartstein M, Horwitz SB. Structural analysis of the mouse *mdr1a* (P-glycoprotein) promoter reveals the basis for differential transcript heterogeneity in multidrug-resistant J774.2 cells. *Mol Cell Biol* 1990;10:3596-606.
- Lepage P, Raymond M, Nepveu A, Gros P. Transcriptional activation of the mouse *mdr3* gene coincides with the appearance of novel transcription initiation sites in multidrug-resistant P388 tumor cells. *Cancer Res* 1993;53:1657-64.
- Raymond M, Gros P. Mammalian multidrug-resistance gene: correlation of exon organization with structural domains and duplication of an ancestral gene. *Proc Natl Acad Sci U S A* 1989;86:6488-92.
- Cohen D, Piekarz RL, Hsu SI-H, DePinho RA, Carrasco N, Horwitz SB. Structural and functional analysis of the mouse *mdr1b* gene promoter. *J Biol Chem* 1991;266:2239-44.
- Huff LM, Lee JS, Robey RW, Fojo T. Characterization of gene rearrangements leading to activation of MDR-1. *J Biol Chem* 2006;281:36501-9.
- Rao PS, Govindarajan R, Mallya KB, West W, Rao US. Characterization of a new antibody raised against the NH₂ terminus of P-glycoprotein. *Clin Cancer Res* 2005;11:5833-9.
- Shi T, Wrin J, Reeder J, Liu D, Ring DB. High-affinity monoclonal antibodies against P-glycoprotein. *Clin Immunol Immunopathol* 1995;76:44-51.
- Kartner N, Evernden-Porelle D, Bradley G, Ling V. Detection of P-glycoprotein in multidrug-resistant cell lines by monoclonal antibodies. *Nature* 1985;316:820-3.
- Barrand MA, Twentyman PR. Differential recognition of *mdr1a* and *mdr1b* gene products in multidrug resistant mouse tumour cell lines by different monoclonal antibodies. *Br J Cancer* 1992;65:239-45.
- Chintamani, Singh JP, Mittal MK, et al. Role of P-glycoprotein expression in predicting response to

- neoadjuvant chemotherapy in breast cancer—a prospective clinical study. *World J Surg Oncol* 2005;3:61.
40. Schinkel AH, Wagenaar E, Van Deemter L, Mol CAAM, Borst P. Absence of the *mdr1a* P-glycoprotein in mice affects tissue distribution and pharmacokinetics of dexamethasone, digoxin, and cyclosporin A. *J Clin Invest* 1995;96:1698–705.
41. Schinkel AH, Borst P. Characterization of the human MDR3 P-glycoprotein and its cross-reactivity with P-glycoprotein-specific monoclonal antibodies. *Cancer Res* 1991;51:2628–35.
42. Georges E, Bradley G, Garipey J, Ling V. Detection of P-glycoprotein isoforms by gene-specific monoclonal antibodies. *Proc Natl Acad Sci U S A* 1990;87:152–6.
43. Schinkel AH, Mayer U, Wagenaar E, et al. Normal viability and altered pharmacokinetics in mice lacking *mdr1*-type (drug-transporting) P-glycoproteins. *Proc Natl Acad Sci U S A* 1997;94:4028–33.
44. Borst P, Rottenberg S, Jonkers J. How do real tumors become resistant to cisplatin? *Cell Cycle* 2008;7:1353–9.
45. Trock BJ, Leonessa F, Clarke R. Multidrug resistance in breast cancer: a meta-analysis of MDR1/*gp170* expression and its possible functional significance. *J Natl Cancer Inst* 1997;89:917–31.
46. Pusztai L, Wagner P, Ibrahim N, et al. Phase II study of tariquidar, a selective P-glycoprotein inhibitor, in patients with chemotherapy-resistant, advanced breast carcinoma. *Cancer* 2005;104:682–91.
47. Van Leeuwen F, Buckle T, Kersbergen A, Rottenberg S, Gilhuijs KG. Non-invasive functional imaging of P-glycoprotein-mediated doxorubicin resistance in a mouse model for hereditary breast cancer to predict response, and assign P-gp inhibitor sensitivity. *Eur J Nucl Med Mol Imaging* 2009;36:406–12.
48. Hendrikse NH, Franssen EJJ, Van der Graaf WTA, et al. ^{99m}Tc -sestamibi is a substrate for P-glycoprotein and the multidrug resistance-associated protein. *Br J Cancer* 1998;77:353–8.
49. Soderberg O, Gullberg M, Jarvius M, et al. Direct observation of individual endogenous protein complexes *in situ* by proximity ligation. *Nature Methods* 2006;3:995–1000.

Cancer Research

The Journal of Cancer Research (1916–1930) | The American Journal of Cancer (1931–1940)

Moderate Increase in *Mdr1a/1b* Expression Causes *In vivo* Resistance to Doxorubicin in a Mouse Model for Hereditary Breast Cancer

Marina Pajic, Jayasree K. Iyer, Ariena Kersbergen, et al.

Cancer Res 2009;69:6396-6404. Published OnlineFirst August 4, 2009.

Updated version

Access the most recent version of this article at:
doi:[10.1158/0008-5472.CAN-09-0041](https://doi.org/10.1158/0008-5472.CAN-09-0041)

Supplementary Material

Access the most recent supplemental material at:
<http://cancerres.aacrjournals.org/content/suppl/2009/07/28/0008-5472.CAN-09-0041.DC1>

Cited articles

This article cites 48 articles, 20 of which you can access for free at:
<http://cancerres.aacrjournals.org/content/69/16/6396.full#ref-list-1>

Citing articles

This article has been cited by 10 HighWire-hosted articles. Access the articles at:
<http://cancerres.aacrjournals.org/content/69/16/6396.full#related-urls>

E-mail alerts

[Sign up to receive free email-alerts](#) related to this article or journal.

Reprints and Subscriptions

To order reprints of this article or to subscribe to the journal, contact the AACR Publications Department at pubs@aacr.org.

Permissions

To request permission to re-use all or part of this article, use this link
<http://cancerres.aacrjournals.org/content/69/16/6396>.
Click on "Request Permissions" which will take you to the Copyright Clearance Center's (CCC) Rightslink site.